Twisting operations in Lyubich-Minsky laminations associated with bifurcations of quadratic maps(Topology, Complex Analysis and Arithmetic of Hyperbolic Spaces)

AUTHOR(S):

Kawahira, Tomoki

数理解析研究所講究録
第1571巻 2007年 155-171

Twisting operations in Lyubich-Minsky laminations associated with bifurcations of quadratic maps

Tomoki Kawahira (川平 友規)
Graduate School of Mathematics
Nagoya University

Abstract

This note gives a brief introduction to Lyubich and Minsky's hyperbolic 3-laminations associated with hyperbolic and parabolic quadratic maps. We will see that a twisting operation naturally appears when a quadratic map bifurcates. This note is based on my talk at RIMS, Kyoto, on 7 December 2006.

1 Introduction: Sullivan's dictionary

1.1 Complex Dynamics

Iteration theory of rational functions. Let $f : \overline{\mathbb{C}} \to \overline{\mathbb{C}}$ be a rational map of $\deg f \geq 2$. For $z_0 \in \overline{\mathbb{C}}$, we consider its *orbit*

$$\overline{\mathbb{C}} \ni z_0 \overset{f}{\longmapsto} z_1 \overset{f}{\longmapsto} z_2 \overset{f}{\longmapsto} \cdots .$$

When we perturb the initial value z_0 a little, the orbit may change slightly (stably), or drastically (unstably). To distinguish the properties of orbits, we define the *Fatou set*:

$$F_f := \big(\text{The maximal open set where } \{f^n\}_{n\in\mathbf{N}} \text{ is normal}\big);$$

which is the domain of stability. (Where f^n is the n times iteration of f). Indeed, we can replace "normal" by "equicontinuous" in the definition. Thus the orbits starting at the Fatou set are stable under perturbation. Its complement $J_f := \overline{\mathbb{C}} - F_f$ gives the unstable orbits. We call J_f the *Julia set*, which is the chaotic locus. Note that F_f and J_f are invariant sets of $f^{\pm 1}$.

Example. $f(z) = z^2 \implies J_f = \mathbb{S}^1$ and $F_f = \overline{\mathbb{C}} - \mathbb{S}^1$. In fact, $f^n \to 0$ or ∞ compact uniformly on F_f as $n \to 0$. By taking a semiconjugacy of f by $w = \phi(z) = z + z^{-1}$, one can check that $g(w) = w^2 - 2$ has $[-2, 2]$ as its Julia set.

1.2 Sullivan's Dictionary

In early 80's, D.Sullivan introduced a dictionary between (finitely generated) Kleinian groups and complex dynamics (iteration theory of rational maps). Here are some of the entries:

f.g. Kleinian gr. $\Gamma \curvearrowright \overline{\mathbb{C}}$	Rational map $f \curvearrowright \overline{\mathbb{C}}$
Domain of disconti. Ω_Γ	Fatou set F_f
Limit set Λ_Γ	Julia set J_f
Fixed points dense in Λ_Γ	Periodic points dense in J_f
Ahlfors finiteness thm.	No wandering domain thm.

Sullivan gave proofs of the two theorems below in the table by using a similar method of the quasiconformal Teichmüller theory. Now our slogan is: *Share methods in both theories!* However, there still are missing entries:

Structurally stable $\Longrightarrow$ expanding	? ($\Longleftarrow$ is known.)
No invariant line field on Λ_Γ	?
Poincaré ext. $\Gamma \curvearrowright \mathbb{H}^3$	No conformal ext. $f \curvearrowright \mathbb{H}^3$
Hyperbolic 3-manifold M_Γ	???

The first two "?"s are affirmatively conjectured and they imply a big result on density of hyperbolic rational maps. To get a new insight for these conjectures, it would be nice for complex dynamics to have a geometric realization like M_Γ of a Kleinian group Γ. So far, the only candidate for "???" below is *Lyubich and Minsky's hyperbolic 3-lamination* $\mathcal{M}_f$ introduced in [LM]. They proved a rigidity theorem of a certain class of rational maps by an analogous argument to Mostow's rigidity theorem and Marden's isomorphism theorem.

Outline of this note. In Section 2, we roughly summerize properties of quadratic maps with connected Julia sets. Section 3 is devoted for a rough sketch of the construction of Lyubich-Minsky laminations. Section 4 gives a worked out example of the Lyubich-Minsky hyperbolic 3-laminations and their degeneration. This note is based on some fundamental facts on complex dynamics. Readers may refer [Mi].

Acknowledgement. This research is partially supported by Inamori Foundation and JSPS.

2 Dynamics of quadratic maps

2.1 Quadratic dynamics and the Mandelbrot set

Let us consider quadratic maps of the form $f(z) = f_c(z) = z^2 + c \quad (c \in \mathbb{C})$. This is enough general, since any quadratic function is affinely conjugate to one of such f_c's.

Basin at infinity. Since $f(z) = z^2(1+c/z^2) \approx z^2$ near ∞, ∞ attracts nearby points. We define the *basin at infinity* by

$$B_f := \{z \in \overline{\mathbb{C}} : f^n(z) \to \infty\} \subset F_f$$

which is an open neighborhood of ∞. Note that B_f is completely invariant, i.e., $f^{\pm 1}(B_f) = B_f$. Here is a classical result on B_f and J_f:

Theorem 2.1 (Fatou, Julia) *For any $f = f_c$, the boundary of B_f coincide with J_f. Moreover, either*

1. *$B_f \cong \mathbb{D} \iff J_f$ is connected; or*
2. *$B_f \ncong \mathbb{D} \iff J_f$ is a Cantor set.*

We define the *Mandelbrot set* by

$$\mathbb{M} := \{c \in \mathbb{C} : B_f \cong \mathbb{D}\}.$$

Now suppose that $B_f \cong \mathbb{D} \iff c \in \mathbb{M}$. Then it is known that there exists a

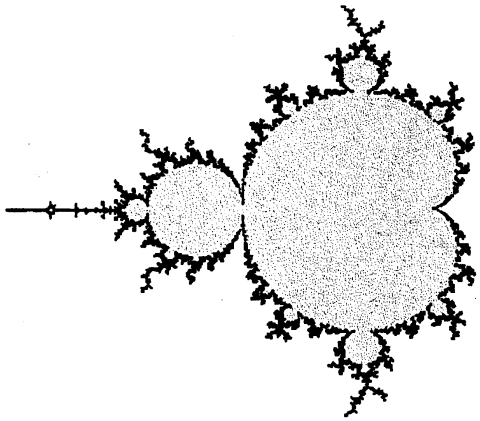

Figure 1: The Mandelbrot set with its boundary emphasized.

unique conformal conjugacy $\Phi_f : B_{f_0} \to B_f$ between the actions $f_0 \curvearrowright B_{f_0}$ and $f \curvearrowright B_f$ satisfying $\Phi_f(z)/z \to 1$ $(z \to \infty)$ (Figure 2). In other words, the dynamics $f \curvearrowright B_f$ we observe is the image of the dynamics of $f_0 : z \mapsto z^2$ acting on $B_{f_0} = \overline{\mathbb{C}} - \overline{\mathbb{D}}$ through a "conformal lens" Φ_f. This is a conformal deformation of the dynamics $f_0 \curvearrowright B_{f_0}$, which gives a quite similar situation to Bers' simultaneous uniformization.

Here is another entry of the dictionary:

The Mandelbrot set $\mathbb{M}$	A Bers slice of $\mathcal{QF}$

Where $\mathcal{QF}$ is the quasi-Fuchsian space, a deformation space of a hyperbolic surface group.

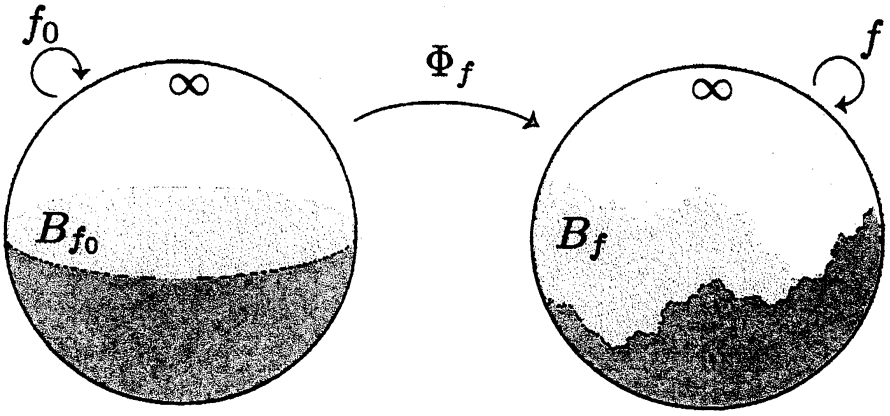

Figure 2: Conformal deformation of the dynamics in B_{f_0}.

2.2 Degeneration v.s. Bifurcation

Let us change the parameter c of $f = f_c : z \mapsto z^2 + c$ from $c = 0$ (small white circle below) as in the curve of Figure 3. It is convenient to define the *filled Julia set* by

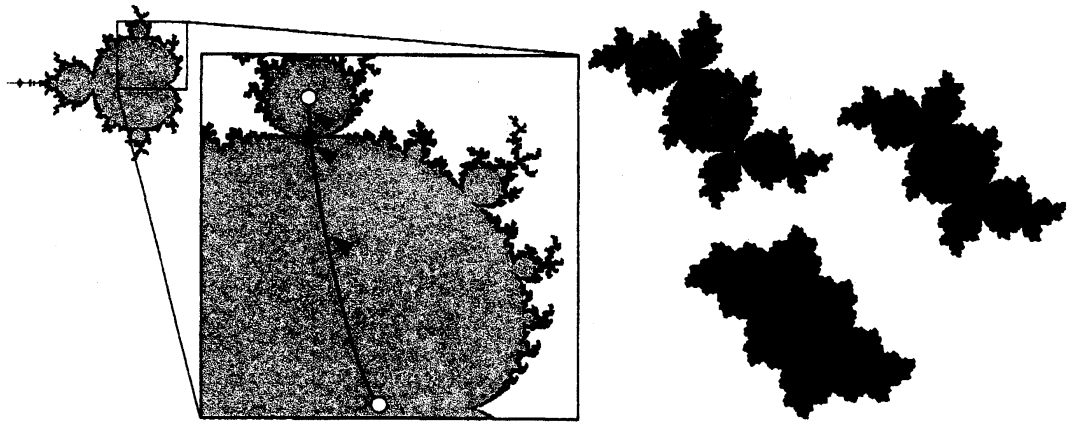

Figure 3: Rabbits

$K_f := \overline{\mathbb{C}} - B_f$. Note that $\partial K_f = J_f$. In Figure 3, the three triangles indicate the parameter c with their filled Julia sets (with some "equipotential curves") drawn on the right. The first one from below, say $f_1 := f_{c_1}$, has an attracting fixed point and its Julia set J_{f_1} is a Jordan curve. The interior of the filled Julia set K_{f_1} is colored in gray. The next one, say $g = f_\sigma$, has a fixed point β with *multiplicity* in the following sense: It is a simple root of the equation $g(z) = z$, but it is a multiple root of $g^3(z) = z$ (in general this equation gives periodic points of period 3) with multiplicity 4. Hence any perturbation of this g causes a bifurcation of this multiple periodic points. The Julia

set J_g is no more a Jordan curve, and K_g° has countably many connected components. The third one, say $f_2 = f_{c_2}$, has periodic points of period three that attract nearby points (the *attracting cycle*). It is known that J_{f_2} is homeomorphic to J_g.

The key to describe the difference between f_1^3, g^3, f_2^3 is the degeneration and bifurcation process with respect to β. f_1 has periodic points of period 3 that repel nearby points (a *repelling cycle*). As the parameter c moves from c_1 to σ, the repelling cycle and the attracting cycle of f_1 merge into one point, β. As the parameter moves from σ to c_2, the degenerated periodic points bifurcate again to be the attracting cycle and the repelling fixed point. Figure 4 shows this process with their nearby dynamics.

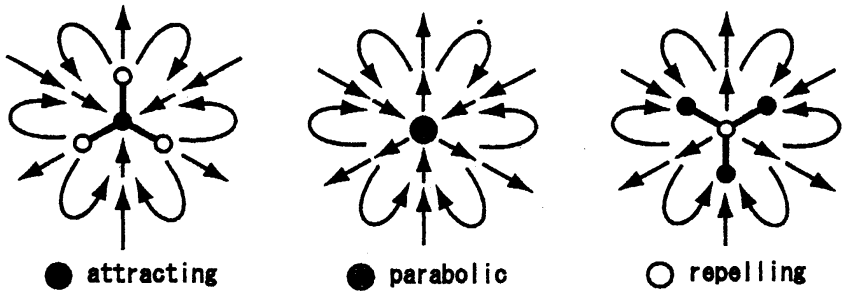

Figure 4: Dynamics of f_1^3, g^3, f_2^3

Let us make the terminology more precise: For a periodic point z of period l, we say $(f^l)'(z)$ is the *multiplier* of z. We also say that z is *attracting* if $|(f^l)'(z)| < 1$, *repelling* if $|(f^l)'(z)| > 1$, and *indifferent* if $|(f^l)'(z)| = 1$. In particular, we say z is *parabolic* if $(f^l)'(z)$ is a root of unity, or equivalently, z is a multiple root of $f^n(z) = z$ for some n. The map $f_c(z) = z^2 + c$ (or the parameter c) is called *hyperbolic/parabolic (parameter)* if f_c has an attracting/parabolic cycle.

By the Douady-Hubbard theory [DH], hyperbolic parameters are determined by the "combinatorics " of the attracting cycles and its multiplier valued in $\mathbb{D}$. Indeed, each connected component of the set of hyperbolic parameters $H \subset \mathbb{M}^\circ$ is isomorphic to $\mathbb{D}$. The boundaries of two of such components may share at most one parabolic parameter. When c moves from one component of H to another, a pair of degeneration and bifurcation process as in Figure 3 happens with various multiplicity of periodic points depending on the parabolic parameter between the two components.

In the following, we try to observe this hyperbolic-to-parabolic degeneration process and parabolic-to-hyperbolic bifurcation process in terms of Lyubich-Minsky laminations. Now let us go to the definition of the Lyubich-Minsky laminations.

3 Lyubich-Minsky laminations

Here we roughly sketch the construction of the Lyubich-Minsky laminations associated with hyperbolic and quadratic maps. Assume: $f = f_c : z \mapsto z^2 + c$, hyperbolic or parabolic. The construction breaks into four steps:

Step1. To get an invertible dynamics, we construct the inverse limit $\mathcal{N}_f = \varprojlim(f, \overline{\mathbb{C}})$ of $f \curvearrowright \overline{\mathbb{C}}$ with lifted action $\hat{f} \curvearrowright \mathcal{N}_f$.

Step2. Take an analytically well behaved part $\mathcal{A}_f \subset \mathcal{N}_f$ which is a Riemann surface ($\mathbb{C}$-)lamination.

Step3. Take an $\mathbb{R}_+$-bundle $\mathcal{H}_f$ of $\mathcal{A}_f$, the $\mathbb{H}^3$-lamination. Then the action $\hat{f} \curvearrowright \mathcal{A}_f$ extends to $\hat{f} \curvearrowright \mathcal{H}_f$.

Step4. The extended action $\hat{f}^{\mathbf{Z}} \curvearrowright \mathcal{H}_f$ is properly discontinuous. Take $\mathcal{M}_f := \mathcal{H}_f/\hat{f}$.

Here is the dictionary:

$\Gamma \curvearrowright \overline{\mathbb{C}}$	$\hat{f} \curvearrowright \mathcal{A}_f$
$\Gamma \curvearrowright \mathbb{H}^3$ prop. distonti.	$\hat{f} \curvearrowright \mathcal{H}_f$ prop. distonti.
$M_\Gamma = \mathbb{H}^3/\Gamma$	$\mathcal{M}_f = \mathcal{H}^3_f/\hat{f}$

3.1 Construction of laminations

Interested readers may refer [LM], [L], and [Ka3, §2]

Step1: Natural extension. First we consider all possible backward orbits in our dynamics. That is, take a point $z_0 \in \overline{\mathbb{C}}$, then choose one of its preimage z_{-1}, and choose one of its preimage z_{-2}, and so on:

$$\overline{\mathbb{C}} \ni z_0 \xleftarrow{f} z_{-1} \xleftarrow{f} z_{-2} \xleftarrow{f} z_{-3} \xleftarrow{f} \cdots$$

We gather all of such backward orbits and consider it a subset of $\overline{\mathbb{C}} \times \overline{\mathbb{C}} \times \overline{\mathbb{C}} \times \cdots$. The *natural extension* of f is

$$\mathcal{N}_f := \left\{ \hat{z} = (z_0, z_{-1}, \ldots) \in \overline{\mathbb{C}}^{\mathbf{N}} \ : \ z_0 \in \overline{\mathbb{C}},\ z_{-n} \xleftarrow{f} z_{-n-1} \right\}$$

There is a big merit to consider the inverse limit: We get an invertible dynamics like Kleninan groups. We define $\hat{f} : \mathcal{N}_f \to \mathcal{N}_f$ as follows:

$$\begin{aligned} \hat{f} : (z_0, z_{-1}, z_{-2}, \ldots) &\longmapsto (f(z_0), f(z_{-1}), f(z_{-2}), \ldots) \\ &= (f(z_0), z_0, z_{-1}, \ldots) \\ \hat{f}^{-1} : (z_0, z_{-1}, z_{-2}, \ldots) &\longmapsto (z_{-1}, z_{-2}, z_{-3}, \ldots) \end{aligned}$$

One can easily check that $\hat{f} : \mathcal{N}_f \to \mathcal{N}_f$ is a homeomorphism. Note that the projection $\pi_f(\hat{z}) := z_0$ semiconjugates $\hat{f}$ and f:

$$\begin{array}{ccccccc} \cdots & \xrightarrow{\hat{f}} & \mathcal{N}_f & \xrightarrow{\hat{f}} & \mathcal{N}_f & \xrightarrow{\hat{f}} & \cdots \\ \downarrow & & \downarrow{\scriptstyle \pi_f} & & \downarrow{\scriptstyle \pi_f} & & \downarrow \\ \cdots & \xrightarrow{f} & \overline{\mathbb{C}} & \xrightarrow{f} & \overline{\mathbb{C}} & \xrightarrow{f} & \cdots . \end{array}$$

Examples.

- $f(z) = z^2 + c$ fixes ∞. Thus $\hat{\infty} := (\infty, \infty, \infty, \ldots) \in \mathcal{N}_f$ satisfies $\hat{f}^{\pm 1}(\hat{\infty}) = \hat{\infty}$.
- Let $\{\alpha_1, \ldots, \alpha_l\}$ be the attracting or parabolic cycle of f, with $f(\alpha_k) = \alpha_{k+1}$ taking subscript modulo l. Then $\hat{\alpha}_k := (\alpha_k, \alpha_{k-1}, \ldots) \in \mathcal{N}_f$ satisfies $\hat{f}^{\pm 1}(\alpha_k) = \hat{\alpha}_{k \pm 1}$.
- If $\hat{z} = (z_0, z_{-1}, \ldots) \in \mathcal{N}_f - \{\hat{\infty}, \hat{\alpha}_1, \ldots, \hat{\alpha}_l\}$ then z_{-n} accumulates on J_f. For example, for any point $z_0 \notin \{0, \infty\}$, any backward orbit by $f_0(z) = z^2$ accumulates on $J_{f_0} = \mathbb{S}^1$.

Remark on Hénon maps. Though it seems the natural extension is an abstract object, it naturally appears in 2-dimensional settings. In [HO], Hubbard and Oberste-Vorth proved that for hyperbolic $f(z) = z^2 + c$, the action $\hat{f} \curvearrowright \mathcal{N}_f - \{\hat{\infty}\}$ is topologically conjugate to $F_{b,c} \curvearrowright J^-$, where $F_{b,c} : (z, w) \mapsto (z^2 + c - bw, z)$ is a complex Hénon map on $\mathbb{C}^2$ with $|b| \ll 1$, and J^- is the backward Julia set of $F_{b,c}$.

Step 2: Affine lamination. Set $\mathcal{A}_f := \mathcal{N}_f - \{\hat{\infty}, \hat{\alpha}_1, \ldots, \hat{\alpha}_l\}$. Note that $\mathcal{A}_f$ is an $\hat{f}$-invariant set. Moreover, the following properties are known:

1. $\mathcal{A}_f$ is a Riemann surface lamination with leaves isomorphic to $\mathbb{C}$.
2. The action $\hat{f} \curvearrowright \mathcal{A}_f$ is a leafwise (complex affine) isomorphism.
3. Every leaf of $\mathcal{A}_f$ is dense in $\mathcal{N}_f$.

We call $\mathcal{A}_f$ the *affine lamination* of f.

Step 3: $\mathbb{H}^3$-lamination. Since each leaf L of $\mathcal{A}_f$ has an complex affine structure isomorphic to $\mathbb{C}$, one can consider a hyperbolic space $\mathbb{H}^3_L$ attached on L. In fact, there exists a natural $\mathbb{R}_+$-bundle $\mathcal{H}_f$ of $\mathcal{A}_f$, which is a 3-lamination with leaves isomorphic to $\mathbb{H}^3$. (See Figure 5.) The construction is one of the most technical part. Roughly put, $\mathcal{H}_f$ is given as a quotient space of the tangent bundle of $\mathcal{A}_f$ (up to rotation of tangent vectors). Here we omit the details.

Step 4: Quotient lamination with boundary. An important fact is: *The leafwise isomorphic (complex affine) action $\hat{f} \curvearrowright \mathcal{A}_f$ extends to a leafwise isometry $\hat{f} \curvearrowright \mathcal{H}_f$.*

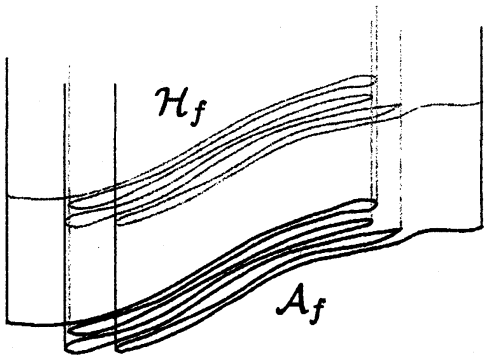

Figure 5: A 1-dimension down caricature of $\mathcal{H}_f$ and $\mathcal{A}_f$

This corresponds to the Poincaré extention. Moreover, *the cyclic group* $\hat{f}^n \curvearrowright \mathcal{H}_f$ *acts properly discontinuously.* Thus $\mathcal{M}_f := \mathcal{H}_f/\hat{f}$ is a Hausdorff space which inherits the hyperbolic 3-laminar structure of $\mathcal{H}_f$. We call $\mathcal{M}_f$ the *quotient lamination* which corresponds to M_Γ of Kleinian group Γ. As hyperbolic 3-manifolds, the quotient laminations may have "conformal boundary" in the following sense: Set $\mathcal{F}_f := (\pi_f|_{\mathcal{A}_f})^{-1}(F_f)$ and $\mathcal{J}_f := (\pi_f|_{\mathcal{A}_f})(J_f)$. These sets give a natural Fatou-Julia decomposition $\mathcal{A}_f = \mathcal{F}_f \sqcup \mathcal{J}_f$:

$$\begin{array}{ccccc} \mathcal{A}_f & = & \mathcal{F}_f & \sqcup & \mathcal{J}_f \\ \downarrow \pi_f & & \downarrow \pi_f & & \downarrow \pi_f \\ \overline{\mathbb{C}} & = & F_f & \sqcup & J_f \end{array}$$

It is known that $\hat{f}$ acts on $\mathcal{F}_f$ properly discontinuously and $\mathcal{F}_f/\hat{f}$ is a Riemann surface lamination. Set $\partial\mathcal{M}_f := \mathcal{F}_f/\hat{f}$, the *conformal boundary* of $\mathcal{M}_f$.

Here are additional entries to the dictionary:

$\Gamma \curvearrowright \Omega_\Gamma$ prop. distonti.	$\hat{f} \curvearrowright \mathcal{F}_f$ prop. distonti.
$\partial M_\Gamma = \Omega_\Gamma/\Gamma$	$\partial\mathcal{M}_f = \mathcal{F}_f/\hat{f}$

Example. Actually $f(z) = f_0(z) = z^2$ (and its perturbation) had been the only well-investigated example(s). In this case F_f is divided into two parts, the basin at infinity $B_f = \overline{\mathbb{C}} - \overline{\mathbb{D}}$ and the basin at zero, $\mathbb{D}$. $\mathcal{B}_f := (\pi_f|_{\mathcal{A}_f})^{-1}(B_f)$ is invariant under the action of $\hat{f}$, and $\mathcal{S}_0 := \mathcal{B}_f/\hat{f}$ is called *Sullivan's solenoidal lamination.* There is a mirror image $\overline{\mathcal{S}}_0$ of $\mathcal{S}_0$ corresponding to $(\pi_f|_{\mathcal{A}_f})^{-1}(\mathbb{D})$. Indeed, $\mathcal{M}_f$ has a product structure $\approx \mathcal{S}_0 \times (0,1)$ that extends to the conformal boundaries. That is, we have $\mathcal{M}_f \cup \partial\mathcal{M}_f \approx \mathcal{S}_0 \times [0,1]$. In [LM] Lyubich and Minsky showed the following:

Proposition 3.1 *If* $f_c(z) = z^2 + c$ *has an attracting cycle (thus* c *is contained in the largest cardioid of* $\mathbb{M}$*) then* $\mathcal{M}_{f_c} \cup \partial\mathcal{M}_{f_c} \approx \mathcal{S}_0 \times [0,1]$.

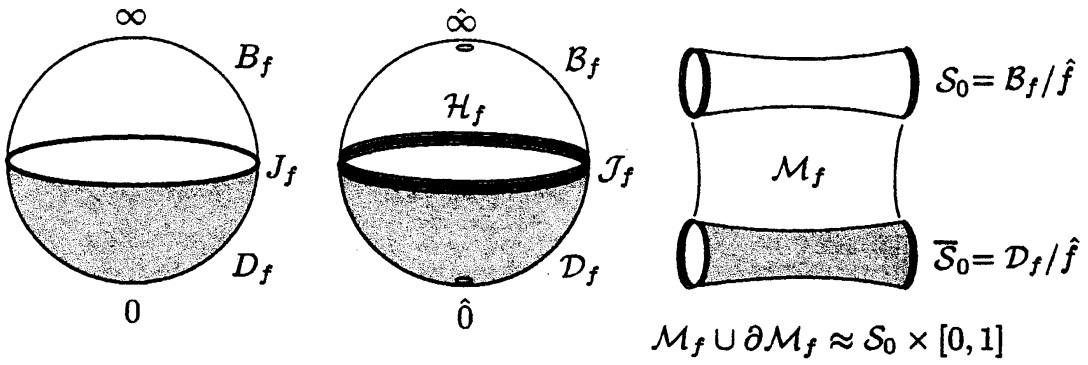

Figure 6: The case of $f = f_0$.

Deformation of f_0. Let us return to a general $f = f_c$ with hyperbolic or parabolic parameter $c \in \mathbb{M}$. Set $D_f := K_f^\circ = \overline{\mathbb{C}} - B_f \cup J_f$ so that $F_f = B_f \sqcup D_f$. Set $\mathcal{B}_f := (\pi_f|_{\mathcal{A}_f})^{-1}(B_f)$ and $\mathcal{D}_f := (\pi_f|_{\mathcal{A}_f})^{-1}(D_f)$. Then we have the corresponding decomposition $\mathcal{F}_f = \mathcal{B}_f \sqcup \mathcal{D}_f$. Note that via $\Phi_f : B_{f_0} \to B_f$, $\mathcal{B}_{f_0}$ and $\mathcal{B}_f$ are conformally identified and so are $\mathcal{S}_0 = \mathcal{B}_{f_0}/\hat{f}_0$ and $\mathcal{B}_f/\hat{f}$. This means that if c of $f = f_c$ moves within $\mathbb{M}$, the structure of $\mathcal{B}_f/\hat{f}$ is conformally preserved. Hence we also denote $\mathcal{B}_f/\hat{f}$ by $\mathcal{S}_0$, and call it the *upper end* of $\mathcal{M}_f = \mathcal{H}_f/\hat{f}$.

On the other hand, the dynamics $f \curvearrowright D_f$ is not preserved by the motion of c; even the topology of D_f changes. In fact, the orbits in D_f are attracted by the attracting or parabolic cycles and the topology of D_f reflects the location and multipliers of these cycles. See Figure 3. The quotient space $\mathcal{S}_f := \mathcal{D}_f/\hat{f}$ upstairs forms a Riemann surface lamination which may have different topology from $\mathcal{S}_0$. We call this end the *lower end* of $\mathcal{M}_f = \mathcal{H}_f/\hat{f}$.

Now we have some more entries[1]:

Fuchsian group Γ of $S = \mathbb{H}/\Gamma$	$f_0(z) = z^2$
$M_\Gamma \cup (\Omega_\Gamma/\Gamma) \approx S \times [0,1]$	$\mathcal{M}_f \cup \partial\mathcal{M}_f \approx \mathcal{S}_0 \times [0,1]$
Deformation of Γ	Deformation of $f_0(z) = z^2$

4 A worked out example (Douady's rabbit)

In this section we mainly deal with f_1, g, f_2 in Section 2 to describe a typical change of the laminations associated with degenerations and bifurcations of hyperbolic quadratic maps. Let us recall the parameters indicated by the two white dots and the three triangles in Figure 3. From bottom to top,

- $f_0(z) = z^2$, hyperbolic with $f_0(0) = 0$.

[1]In general a family of rational maps called *Blashcke product* corresponds to the family of Fuchsian group.

- $f_1(z) = z^2 + c_1$, hyperbolic with an attracting fixed point of multiplier $r_1 e^{2\pi i/3}$ for some $0 < r_1 < 1$.
- $g(z) = z^2 + \sigma$, parabolic with parabolic fixed point of multiplier $e^{2\pi i/3}$.
- $f_2(z) = z^2 + c_2$, hyperbolic with an attracting cycle of period three whose multiplier is $0 < r_2 < 1$.
- $f_3(z) = z^2 + c_{\mathrm{rab}}$, hyperbolic with $f_3^3(0) = 0$. (Its Julia set is called "Douady's rabbit".)

One may expect some topological difference between $\mathcal{M}_{f_0}$ and $\mathcal{M}_{f_3}$ but there had been no investigations before the author's work [Ka2] and [Ka3]. Here we describe the difference along the arguments of these papers.

Stability of hyperbolics. First we consider the difference between the laminations of f_0 and f_1 (or f_2 and f_3). It is known that they have quasi-conformally the same dynamics near the Julia sets but the whole dynamics are different. The Lyubich-Minsky laminations have a similar property to the Julia sets. We have:

Theorem 4.1 ([Ka3]) *The dynamics $f_0 \curvearrowright \mathcal{A}_{f_0} \cup \mathcal{H}_{f_0}$ and $f_1 \curvearrowright \mathcal{A}_{f_1} \cup \mathcal{H}_{f_1}$ are conjugate. Indeed, we can take a conjugacy which is leafwise quasiconformal on the affine laminations and leafwise quasi-isometry on the hyperbolic laminations. Moreover, $\mathcal{M}_{f_0} \cup \partial\mathcal{M}_{f_0}$ is homeomorphic to $\mathcal{M}_{f_1} \cup \partial\mathcal{M}_{f_1}$. The same holds for f_2 and f_3.*

So it is enough to compare f_1, g, and f_2.

4.1 Degeneration of rabbits

First we describe the difference between the dynamics downstairs. If r_1 and r_2 tend to 1, f_1 and f_2 tends to g. They are two distinct process of degeneration. It is convenient to use *external rays* to describe these process. Since the dynamics of B_{f_1}, B_g, and B_{f_2} (the basins at infinity) are conformally the same as B_{f_0}, we can pull-back the foliation on B_{f_0} by the radial rays (which is invariant under the dynamics of f_0) to each basin at infinity. In general, when K_f is connected, we define *the external ray of angle $\theta \in \mathbb{R}/\mathbb{Z}$* by

$$R_f(\theta) := \Phi_f(\{re^{2\pi i\theta} : r > 1\}).$$

Then we have $f(R_f(\theta)) = R_f(2\theta)$.

From f_1 to g. It is known that the parabolic fixed point β of g is the landing point of the external rays of angles $1/7, 2/7$ and $4/7$. For f_1, the landing points of the external rays of angle angles $1/7, 2/7$ and $4/7$ are all distinct and form a repelling periodic cycle. As f_1 tends to g, the attracting fixed point of f_1 and the repelling cycle degenerate into one parabolic fixed point β. See Figure 4, from the left to the middle.

In this case, we can find an f_1-invariant graph that joins the central attracting fixed point and the repelling cycle. we denote it by I_1 (Figure 7).

From f_2 to g. In the case of f_2, the external rays of angles $1/7, 2/7$ and $4/7$ land at the same repelling fixed point. As f_2 tends to g, the repelling fixed point and three attracting periodic point degenerate into one parabolic fixed point β. See Figure 4, from the right to the middle.

We can also find an f_2-invariant graph that joins the central repelling fixed point and the attracting cycle. we denote it by I_2 (Figure 7).

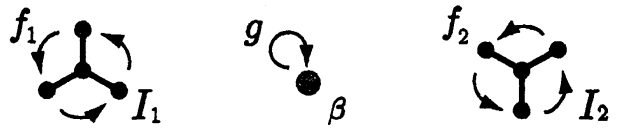

Figure 7: The invariant arcs I_1 and I_2.

Now we set $I_{f_i} := \bigcup f_i^{-n}(I_i)$ for $i = 1, 2$, and $I_g := \bigcup g^{-n}(\{\beta\})$. Figure 8 shows the filled Julia sets of K_{f_i} with I_{f_i} drawn in. As we will justify in Theorem 4.3, we may consider that the dynamics of g is given by just pinching I_{f_i} to I_g.

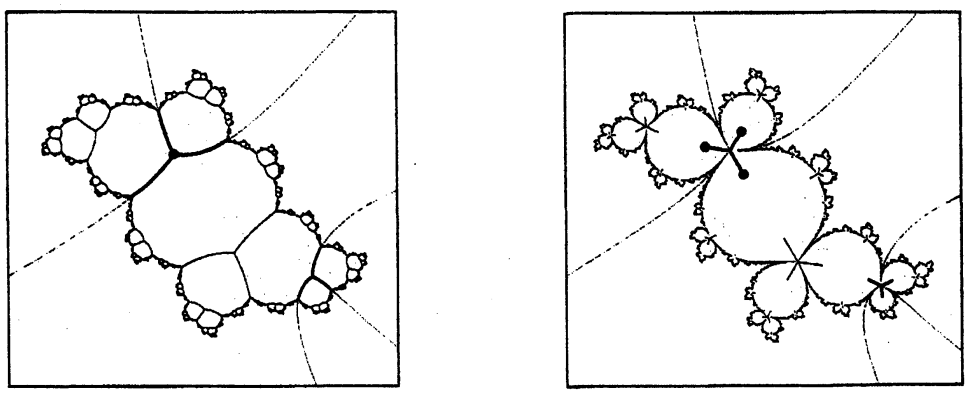

Figure 8: The external rays of angles $\{1/7, 2/7, 1/7\}$ and $\{1/28, 23/28, 25/28\}$ are also drawn in.

Tessellation. The dynamics on B_f (the basin at infinity, "outside" the Julia sets) is perfectly organized by the external rays and their relation $f(R_f(\theta)) = R_f(2\theta)$. On the other hand, dynamics on D_f ("inside" the Julia sets) are or perfectly organized by *tiles*.

Theorem 4.2 ([Ka2]) *For $i = 1, 2$, $D_{f_i} - I_{f_i}$ and $D_g = D_g - I_g$ are tessellated by tiles of the from $T_\circ(\theta, m, *)$ with $\circ = f_i$ or g, $\theta \in \mathbb{Q}/\mathbb{Z}$, $m \in \mathbb{Z}$, $* = +$ or $-$ satisfying the following.*

- *Each tile has a topological disk as its interior.*
- *f_i maps $T_{f_i}(\theta, m, \pm)$ to $T_{f_i}(2\theta, m+1, \pm)$ homeomorphically.*
- *g maps $T_g(\theta, m, \pm)$ to $T_g(2\theta, m+1, \pm)$ homeomorphically.*
- *$T_{f_i}(\theta, m, *)$ and $T_{f_i}(\theta', m', *')$ share their boundary points iff so do $T_g(\theta, m, *)$ and $T_g(\theta', m', *')$.*

Figure 9 shows the tessellations for f_1 and f_2. It is difficult to draw a nice picture of the tessellation for g because moire appears. But one can imagine it by pinching I_{f_i}.

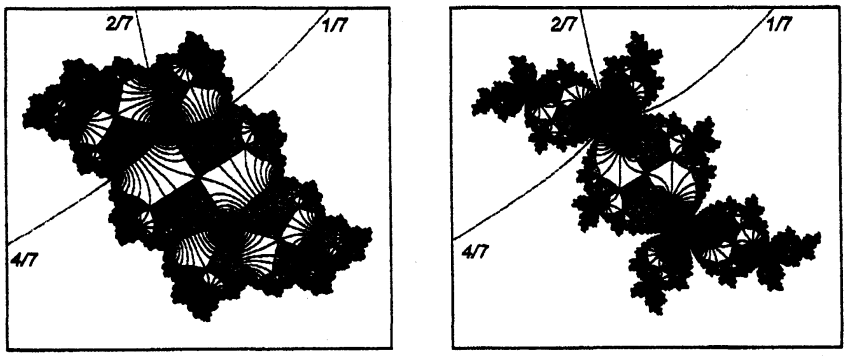

Figure 9: The tessellations for f_1 and f_2.

Actually the parameters θ of tiles are closely related to the angles of external rays but here we omit the details. Interested readers may refer [Ka2].

Pinching semiconjugacies. By using tessellations, we have:

Theorem 4.3 ([Ka2]) *For $i = 1, 2$, there exists a continuous and surjective map $h_i : \overline{\mathbb{C}} \to \overline{\mathbb{C}}$ such that:*

1. *h_i is a semiconjugacy. That is, $f_i \circ h_i = h_i \circ g$.*
2. *h_i sends I_{f_i} onto I_g. In particular, if $\operatorname{card} h_i^{-1}(y) \geq 2$ then $y \in I_g$.*
3. *h_i sends $T_{f_i}(\theta, m, \pm)$ to $T_g(\theta, m, \pm)$ homeomorphically.*
4. *$h_i|_{B_{f_i}} = \Phi_g \circ \Phi_{f_i}^{-1}$ and it conformally conjugates $f_i \curvearrowright B_{f_i}$ to $g \curvearrowright B_g$.*
5. *h_i sends J_{f_i} onto J_g. Moreover, it is a conjugacy when $i = 2$.*
6. *$h_i \to \mathrm{id}$ as $f_i \to g$.*

So we can describe the dynamics of g downstairs by that of f_i by means of the semiconjugacies. We can lift the semiconjugacies to the objects (laminations) upstairs.

4.2 Degeneration of laminations

First we roughly describe the degeneration of the affine laminations. By lifting the semiconjugacy $\hat{h}_i$ $(i = 1, 2)$ to the affine laminations $\mathcal{A}_{f_i}$ and $\mathcal{A}_g$, we can precisely describe the difference. The lift is explicitly given by:

$$\hat{h}_i : (z_0, z_{-1}, \ldots) \longmapsto (h_i(z_0), h_i(z_{-1}), \ldots).$$

It is convenient to consider the *principal* and *non-principal part* of the affine laminations. The *principal part* Λ_{f_i} and Λ_g of $\mathcal{A}_{f_i}$ and $\mathcal{A}_g$ are the sets of backward orbits accumulating on f_i-invariant arc I_i and the parabolic fixed point β respectively. The rest is called the *non-principal part.*

Affine laminations: Non-principal part. The lifted semiconjugacy $\hat{h}_i$ $(i = 1, 2)$ sends the non-principal part of $\mathcal{A}_{f_i}$ to the non-principal part of $\mathcal{A}_g$. Since h_i just pinches I_{f_i} to I_g, its natural lift $\hat{h}_i$ on the non-principal parts pinches the backward orbits within I_{f_i} to those within I_g. As in Figure 10, such a pinching does not change the structure of leaves so the non-principal part have no significant difference.

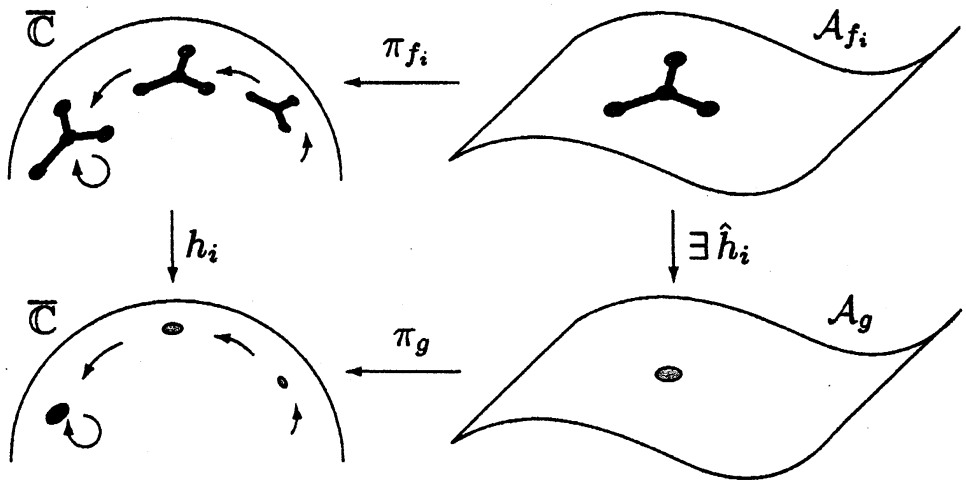

Figure 10: Pinching map in the non-principal part

Affine laminations: Principal part. In the principal parts we have a difference of topologies. Figure 11 shows the dynamics near I_i $(i = 1, 2)$ and β, and their corresponding principal parts.

The principal part Λ_{f_1} consists of the three cyclic leaves corresponding to the repelling periodic points of period three. One can regard the action on these leaves as hyperbolic affine maps by taking suitable uniformizations of leaves.

The principal part Λ_g also consists of the three cyclic leaves corresponding to the repelling directions of the parabolic fixed point. One can regard the action on these

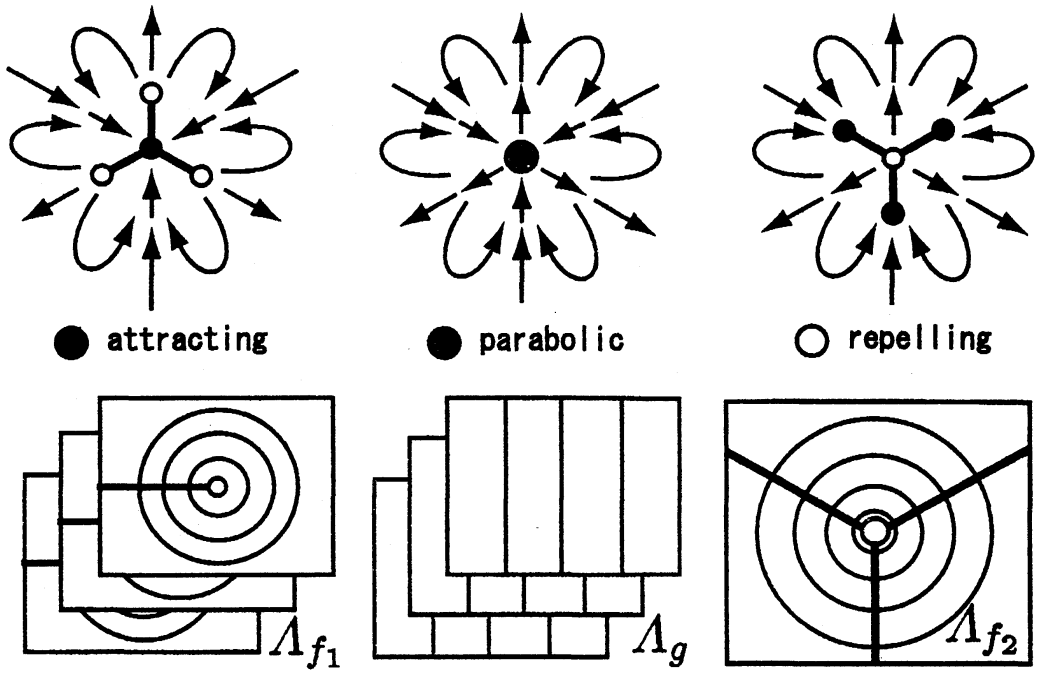

Figure 11: The principal part and corresponding dynamics downstairs.

leaves as parabolic affine maps (translations) by taking suitable uniformizations of leaves. Recall that the backward orbit $\hat{\beta} = (\beta, \beta, \beta, \ldots)$ is irregular so we can not find it in the affine lamination.

The principal part Λ_{f_2} consists of one invariant leaf corresponding to the repelling fixed point. One can also regard the action on this leaf as a hyperbolic affine map by taking a suitable uniformization.

The thickened curves in the leaves shows the lift of f_i-invariant graph I_i. By the lift $\hat{h}_i$ of the pinching map h_i, the thickend curves are pinched to the irregular point $\hat{\beta}$. (Observers in the affine laminations may say that the curves are just pushed away to infinity.) This causes the topological or dynamical difference between the principal parts of the affine laminations. See Section 5 of [Ka3] for more details.

$\mathbb{H}^3$-laminations. Next we consider the $\mathbb{H}^3$-laminations. Since the $\mathbb{H}^3$-lamination is an $\mathbb{R}_+$-bundle of the affine laminations, we can extend the pinching map $\hat{h}_i$.

As in the affine laminations, the 3-dimensional extension of the non-principal parts have no significant difference. The difference of the 3-dimensional extension of the principal parts are described in a similar way (Figure 12). See Section 6 of [Ka3] for more details. Here we just note that the action of $\hat{f}_i$ (resp. $\hat{g}$) on the 3-dimensional extension $\Lambda^{\mathrm{h}}_{f_i}$ (resp. Λ^{h}_g) of Λ_{f_i} (resp. Λ_g) is loxodromic (resp. parabolic).

Quotient laminations. Finally let us consider the quotient laminations. For $\mathcal{M}_{f_i}$ $(i = 1, 2)$ and $\mathcal{M}_g$, we define their principal parts by the quotient of 3-dimensional

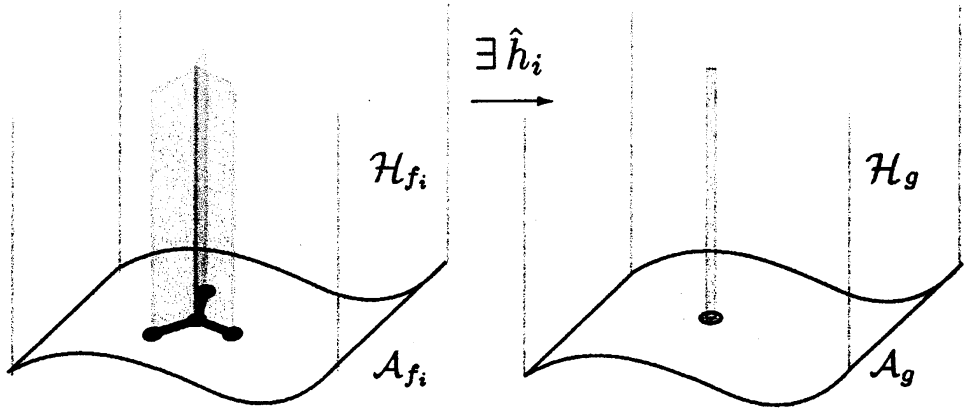

Figure 12: Pinching $\mathbb{H}^3$-leaves.

extensions of the principal parts by the dynamics. Then we have *solid tori* $\ell_{f_i} \subset \mathcal{M}_{f_i}$ associated with $\hat{f}_i \curvearrowright \Lambda^{\mathrm{h}}_{f_i}$ $(i = 1, 2)$ and a *rank one cusp* $\ell_g \subset \mathcal{M}_g$ associated with $\hat{g} \curvearrowright \Lambda^{\mathrm{h}}_g$ as the principal parts (leaves) of the quotient laminations.

Since $\hat{h}_i$ on the 3-dimensional extensions of the non-principal parts is a semiconjugacy, we have:

Theorem 4.4 (Non-principal part) *$\mathcal{M}_{f_1} - \ell_{f_1}$, $\mathcal{M}_g - \ell_g$, and $\mathcal{M}_{f_2} - \ell_{f_2}$ are all homeomorphic.*

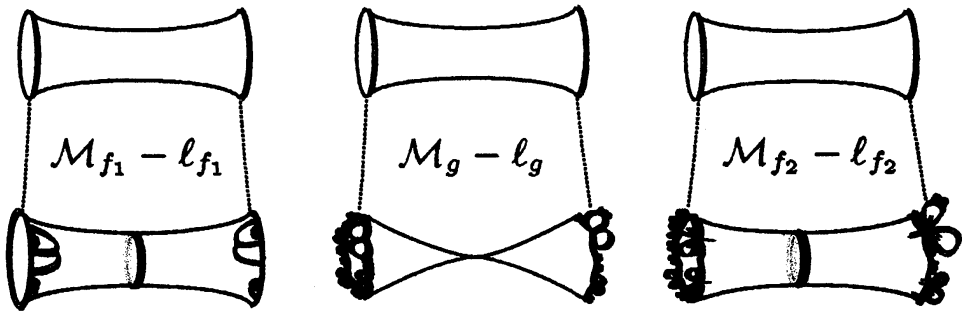

Figure 13: Non-principal parts of the quotient laminations

So the main difference may appear in the principal part. Note that a solid torus and a rank one cusp have topologically the same interior. Moreover, the upper ends of the principal leaves come from conformally the same dynamics in the basins at infinity. Thus the topological difference is given by the lower ends in the principal leaves.

By investigating the structures of the lower ends by lifting tiles downstairs, we can describe the difference of the lower ends as follows (Figure 14.):

- The lower end of ℓ_{f_1} is an annulus with the lift of I_{f_i}. There is a simple closed curve that corresponds to the backward orbits remained on I_1.
- As I_{f_i} is pinched to I_g, the lower end changes its topology. The lower end of ℓ_g has countably many components with only two cuspidal parts.
- The lower end of ℓ_{f_1} also has countably many components with only one annular component. There is also the lift of I_{f_2}. There is a simple closed curve on the annular component that corresponds to the backward orbits remained on I_2.
- In particular, compared with the lower end of ℓ_{f_1}, that of ℓ_{f_2} is *(combinatorially)* 1/3-*twisted* along the simple closed curve corresponding to I_1. Here "1/3-twisted" means that there are three tiles along the curve and the connection of tiles are twisted by the amount of one tile.

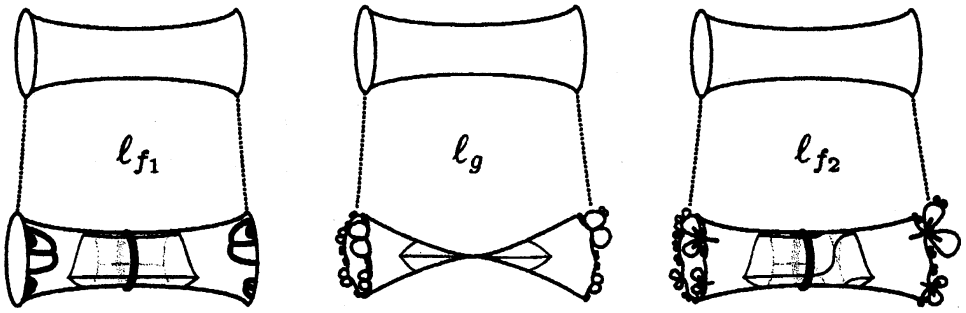

Figure 14: Principal parts of the quotient laminations

Remarks.

1. The case we dealt with is the case when the parameter c of $f = f_c$ moves from 0 to the center of the 1/3-limb of the Mandelbrot set. More generally, when it moves into p/q-*limb*, the lower end is (combinatorially) $\tilde{p}/q$-twisted with $\tilde{p}p \equiv 1 \mod q$.
2. By similar observations, when the parameter c continuously moves from 0 to other components of $\mathbb{M}^\circ$ via parabolic parameters, the interior of the quotient lamination is topologically preserved. After infinitely many degenerations and bifurcations, the parameter will converges to a parameter that gives so-called an *infinitely renormalizable quadratic map*. It seems natural to expect that the quotient lamination of such a map has topologically the same interior as that of f_0, but its lower end is totally degenerate. Here is an interesting question: Can one define the "end invariants" to distinguish the quotient laminations of infinitely renormalizable maps?

References

[DH] A. Douady and J. H. Hubbard. *Etude dynamique des polynômes complexes I & II.* Pub. Math. d'Orsay 84–02, 85–05, 1984/85.

[HO] J.H. Hubbard and R.W. Oberste-Vorth. Hénon mappings in the complex domain II: projective and inductive limit of polynomials. *Real and Complex Dynamical Systems*, B. Branner (ed.) et al., *NATO Adv. Sci. Inst. Ser. C. Math. Phys. Sci.*, **464**, Kluwer Acad. Publ., 1995.

[KL] V.A. Kaimanovich and M. Lyubich. Conformal and harmonic measures on laminations associated with rational maps. *Mem. Am. Math. Soc.*, **820**, 2005.

[Ka1] T. Kawahira. On the regular leaf space of the cauliflower. *Kodai Math. J.* **26** (2003) 167–178.

[Ka2] T. Kawahira. Tessellation and Lyubich-Minsky laminations associated with quadratic maps I: Pinching semiconjugacies. Preprint, 2006. (arXiv:math.DS/0609280)

[Ka3] T. Kawahira. Tessellation and Lyubich-Minsky laminations associated with quadratic maps II: Topological structures of 3-laminations. Preprint, 2006. (arXiv:math.DS/0609836)

[L] M. Lyubich. Laminations and holomorphic dynamics. *Lecture notes in "New Direction in Dynamical Systems"*, Kyoto, 2002.

[LM] M. Lyubich and Y. Minsky. Laminations in holomorphic dynamics. *J. Differ. Geom.* **47** (1997), 17–94.

[Mi] J.Milnor. *Dynamics in one complex variable (3rd edition).* Annals of Math Studies 160, Princeton University Press, 2006.